Contents lists available at **CEPM**

Computational Engineering and Physical Modeling

Journal homepage: www.jcepm.com

Static Analysis of Rigid Airfield Pavement Using Finite Element Method Vs Closed-Form Solution

K. Kavin Mathi[1], K. Nallasivam[2]*

1. PG Student of Transportation Engineering, Department of Civil Engineering, National Institute of Technology (NIT) Hamirpur, Himachal Pradesh, India
2. Assistant Professor of Department of Civil Engineering, National Institute of Technology (NIT) Hamirpur 177001, Himachal Pradesh, India
Corresponding author: *nallasivam@nith.ac.in*

https://doi.org/10.22115/CEPM.2023.354941.1219

ARTICLE INFO

Article history:
Received: 05 August 2022
Revised: 11 April 2023
Accepted: 20 April 2023

Keywords:
Rigid airfield pavement;
Static analysis;
Finite element;
Closed-Form Solution.

ABSTRACT

In addition to the geometry of runway design, a good runway should also meet the structural requirements. In this way, the analysis and design of pavement slabs need to be given more attention. The study looks at the static analysis of a 3D-modeled concrete slab resting on a subgrade foundation that is a homogeneous, isotropic elastic half-space model. This is done so that the effect of a change in Young's modulus can be compared to Winkler's reaction modulus. ANSYS's finite element software, which models the slab as a 3D element with 8 nodes and a solid 185-element type, is used to estimate the combined stresses caused by the weight of the plane and the temperature difference. Conventional slab analysis is done using modified Westergaard's allowable stress method and Eisenmann's method (warping stresses). This is because the two aircraft on the slab have different structural parameters, like the concrete's elasticity modulus, slab thickness, and temperature gradients. From both the outside and inside landing gear loading positions, the maximum values of bending tensile stress were found to go up a lot as the elastic modulus and compressive strength of concrete went up, but they went down at the same time as the thickness of the pavement slab went up. When both + and - temperature gradients were measured on the slab, the corner moved more than the centre. When it comes to stress, a positive curling temperature gradient is worse than a negative curling temperature gradient.

How to cite this article: Mathi KK, Nallasivam K. Static analysis of rigid airfield pavement using finite element method vs closed-form solution. Comput Eng Phys Model 2022;5(4):23–50. https://doi.org/10.22115/cepm.2023.354941.1219

1. Introduction

The transportation industry is one of the industries that provide the most essential element to the country's establishment and economic growth. The demand for airports that meet international standards has grown all around the globe. These high-weight modified generational aircraft with varying landing gear configurations have also presented various issues to civil engineers since they primarily influence traditional airport pavement design processes. The critical stress condition, which is the ultimate flexural bending stress that develops in the slab as a function of wheel load and temperature, governs the structural performance of the airport pavement. Rigid pavements are examined using elastic theory, with the assumption that the pavement is a plate of elastic material resting on top of a foundation which is either elastic or viscous. To provide improvement for additional aircraft, the design process should take into account several approaches to increase the structural capacity of the structure. To achieve this goal, one of three parameters may be changed: the flexural bending strength of the concrete, the slab thickness, or the load transfer effectiveness of the joint. Most airports currently use M40 grade concrete, which is classified as standard or conventional strength and has a flexural strength of 40 kg/cm2. For a given joint spacing, thicker slabs are found to have less curl stress than thinner slabs. Though the increment in slab thickness by a confined amount has a nominal effect on the overall pavement cost, there is a significant increase in pavement life. Even increasing the concrete flexural strength will result in improved pavement performance in terms of its fatigue life, but increasing the slab thickness is found to be more cost-effective. Providing a good base or sub-base layer also increases the pavement's life considerably. The behaviour of stiff airfield runways to a moving aircraft and a temperature difference throughout the depth is investigated using a finite element-based dynamic analysis technique. The viscoelastic subgrade is suitable. The spring and dashpot suspensions model the aircraft's traverse. A parametric study investigates the impacts of individual factors on the rigid airport pavement dynamic response [1]. The research report entitled "Influence of slab size on rigid airport pavement performance investigated by the effect on maximum bending stress in joints", made software model simulations and the results which were obtained from ILLISLAB, JSLAB 92, and Westergaard's method were compared [2]. The static behaviour of pavements to moving vehicle and aeroplane loads has piqued the attention of pavement and runway designers in recent years. This paper presents a finite element-based approach for static analysis of moving vehicle or aircraft stresses on rigid pavements. To model infinity boundary circumstances, the concrete pavement employs finite and infinite beam elements. Pasternak models the underlying soil media, enabling spring shear interaction. Connecting spring elements to elastic deformation vertical elements that deform in transverse shear may achieve this. Assuming isotropic shear layer deformations and forces, equilibrium is maintained. The effect of moving load position on pavement response is investigated and parameterized [3]. The FAA's runway pavement thickness design steps depend largely on load transfer. Under static and moving aeroplane gear, load transmission across a joint differs. The impact of differential stress distribution along the joint was examined using FEAFAA, a 3D finite element analysis tool [4]. The research analyses airport concrete pavement's dynamic deflection and velocity response to impact loads. The influence of an aeroplane's landing weight related to vertical landing acceleration is explored in this research. Using the solution, a

MATLAB application is created to analyze system parameters [5]. During landing, the investigative aircraft places significant stress on the runway. The applied load is determined by the aircraft's weight and vertical velocity before impacting the landing spot. Similarly, the performance of runway pavement is influenced by a variety of factors such as the number of landings, load factor, soil qualities, and so on. Landing procedures, imposed load analysis, and runway pavement evaluation are all part of this study. The study focuses on the idealization of runway characteristics using mechanical components, implying that the mechanical modelling approach might be utilised to anticipate runway deflection [6]. Given the significance of airports and the necessity to improve runways, the research provided pavement response values under varying aircraft loads by utilizing tyre and pavement modelling using a finite element method (FEM). To anticipate the specific actions of pavements under aeroplane loading, ABAQUS was applied. The approach determines pavement stress and deflection at different speeds using finite element analysis and software modeling [7]. The framework and results based on rapid 3D FEM prediction models are provided, as well as notable findings and recommendations for using the developed models in the structural design and evaluation of rigid airport pavement systems. The created models correctly predicted 3D FEM pavement solutions for all cases in this work, could account for stiff pavement foundation-related distresses, and might be employed in the future as surrogate forward response prediction models in FAIRFIELD [8]. Using field data and a 3D FEM model, the analysis was centred on normal vs. winter weather airport rigid pavement under aeroplane loads, temperature loads, and their interaction effects. The effects of interfacial interaction on pavement reactions are being modelled and discussed [9]. The effects of changing daily temperatures on concrete pavement Large temperature variations and traffic volume may lead concrete slabs to exceed their flexural tensile strength, resulting in pavement degradation. Researchers calculated ultimate tensile stresses in concrete slabs of various sizes, thicknesses, and length /width ratios using the finite element (FEM) method. Flexural tensile strength and fatigue life are critical pavement construction features. The ideal slab size and critical thickness were determined by comparing maximum tensile stress and fatigue limit [10]. Pavement thickness design and lifespan estimation are compared in the stiff aircraft pavement. The large disparity between pavement design and life prediction explains why stiff aircraft pavement life spans outperform conventional structural design lifetimes. The pre-compaction process was modelled using a combined FEM cum DEM approach in the paper. To investigate the impacts of asphalt mix gradation, a densely graded asphalt mixture and a gap-graded asphalt mixture were simulated. Several paving speeds were used in the preliminary compaction model to evaluate the influence of paving speeds on the compaction process [11]. Using artificial neural networks, genetic programming, and the Combinatorial Group Method of Data Handling, the researchers developed and validated machine learning-based prediction models for dynamic modulus (E*) of hot mix asphalt [12]. Established 3D FE M models of SCB specimens, as well as a collection of 2D FEM models built from unique slice photos collected by X-ray CT scanning. Using 3D FEM analysis and experimental testing results, the influence of aggregate distribution, aggregate size, mortar content, and other interior structural parameters on the 2D FEM study conclusions was investigated [13]. The Contact Dynamics technique is proposed to analyse the contact system by combining the finite element method (FEM) with the discrete element method. FEM is used to simulate the tyre and capture the resulting contact stresses on the pavement surface, while DEM

is used to simulate the heterogeneous structure of an asphalt mixture and analyse internal mixture reactions at the particle level. The work improved and extended mesh-based methodologies for analysing pavement surface degradation under tyre stresses, which might help with pavement surface design [14].

2. Research significance

For this paper and based on the recent requirement of improved structural adequacy, various landing gear loads which include that of heavy aircraft are considered. The research concentrates on determining structurally appropriate concrete pavement thickness for the planned runway using finite element modelling and static analysis. The scope of the effort to meet the aforementioned goals is as follows:

- To find out the initial reference thickness that is structurally capable of handling heavy aircraft as per the guidelines of FAA and PCA.
- To compare the static load stresses from modified Westergaard's method and finite element model (FEM) using ANSYS for the significant aircraft considered.

A variety of variables influence the structural behaviour of rigid airfield pavement, including

- Concrete slab properties such as its dimensions, joint spacing, flexural strength, modulus of elasticity, fatigue life, coefficient of thermal expansion, Poisson's ratio and shrinkage.
- Aircraft load distribution between each axle group and the distance between the axles in the given group, speed of vehicular loads (dynamic analysis) and traffic wander. Frequency of loading, suspension system tyre inflation.
- Miscellaneous properties such as the sub-base and subgrade characteristics which include the Poisson's ratio, angle of internal friction strength and thickness, presence of dowel bars, pavement roughness and air traffic during the design period also play a major role.

3. Study areas

The research approach is used at Mangalore International Airport in Karnataka (Fig. 1), India, to accommodate wide-body aircraft such as the Boeing 777 and Airbus 380. The asphalt and concrete runways are 1,615m and 2,450m long, respectively, with magnetic directions of 09/27 and 06/24. The impacts of two aeroplanes, the A380 and the B747, as well as varied subgrade bearing strengths and temperature gradients, were researched. Coupled stresses due to aeroplane load and temperature difference were correctly computed and compared using the finite element software, ANSYS. The variations in stress levels caused by the two aircraft were calculated. The findings of the finite-element simulation are also used to construct a simpler approach for estimating maximum stresses. This prediction approach is a handy tool for estimating stresses at the early stages of design. The suggested equations need changes to Westergaard's load stress

model and Eisenmann's temperature stress model, as well as modifications to the independent actions of load and temperature.

Fig. 1. Mangalore Airport Graphic Represents Current Runways and Future Development Runway.

4. Methodology

4.1. Static analysis of the proposed pavement

Static analysis of pavement depends on the position and magnitude of load in addition to the warping and curling effects due to temperature variation. Static analysis by the FAA method considers edge loading conditions whereas the PCA method for pavement design considers interior loading conditions.

4.1.1. Determination of initial reference thickness - FAA method

The FAA design curves need four design input parameters: concrete flexural strength, modulus of subgrade response (k), gross weight of design aircraft, and yearly departure of design aircraft. Terminal Area Forecasts, Airport Activity Statistics, and IATA's Air Traffic Activity might all be used to anticipate annual departures by aircraft type. The yearly departure prediction includes a range of aircraft, with the design aircraft requiring the most pavement thickness. Eq(1) yields the corresponding yearly departures by design aircraft, where the conversion factors in terms of design aircraft landing gear arrangement are determined from Table 1. The maximum expected take-off gross weight of the aircraft is used, considering additional fuel weight. The main landing gears are expected to carry 95 % of the overall weight, with the nose gear carrying the remainder. The distribution of tyre load and the reaction to the pavement are affected by the gear type combinations, which include Single Geared, Dual Geared, Dual Tandem Geared, and Wide

Body aircraft. The following relationship is used to calculate the equivalent repetition of numerous loads.

$$Log\ \mathbf{R}_1 = Log\ \mathbf{R}_2 \left(\frac{W_2}{W_1} \right)^{0.5} \tag{1}$$

Where

R_1 = Design aircraft equivalent annual departure

R_2 = Yearly departures represented in aeroplane landing gear design

W_1 = Design aircraft's wheel load

W_2 = Wheel load of the aircraft in consideration

Tire pressure is affected by gear design and gross weight. A pavement thickness at high-speed turnoffs is 0.9T and at unlikely traffic at the extreme outer edges of runways is 0.7 T, where T is the total thickness obtained from design curves.

Table 1
Factor to Convert to Critical Aircraft Landing Gear Configuration.

To Convert From	To	Multiply Departures by
single wheel	dual wheel	0.8
single wheel	dual tandem	0.5
dual wheel	dual tandem	0.6
double dual tandem	dual tandem	1.0
dual tandem	single wheel	2.0
dual tandem	dual wheel	1.7
dual wheel	single wheel	1.3
double dual tandem	dual wheel	1.7

Source: FAA/AC-150/5320-6C (revised by FAA advisory circular)

Table 2
Recommended Maximum Joint Spacing for Rigid Pavement.

Stabilised sub-base		Stabilised sub-base	
Slab Thickness, *h*(mm)	Joint Spacing, *l* (m)	Slab Thickness, *h*(mm)	Joint Spacing, *l* (m)
203-254	3.8	152	3.8
267-330	4.6	165-229	4.6
343-406	5.32	>229	6.1
>406	6.1	-	-

Source: FAA-Advisory Circular 150-53206E.

Slabs supported by a stabilised subbase experience more warping and curling pressures than those supported by unstabilized foundations. Table 2 shows the joint spacing in the longitudinal

axis for both cases. In both circumstances, the ratio of the longest side of a slab to the shortest side of a slab at two crossing sides should not be more than 1.25 in non-reinforced pavements. The trial thickness 'h' is found from the design curves corresponding to the present design aircraft A-310. This thickness is fed into the PCA method's fatigue check to find its structural adequacy. The annual departure in terms of future design aircraft A-380 is also found which could be used for further study. Trial thicknesses are chosen for further study Fig. A1 depicts the flowchart (APPENDIX-A).

4.1.2. Check for structural adequacy - PCA method

PCA method involves the concept of fatigue failure on account of mixed air traffic. The initial trial slab thickness is assumed preferably from the FAA method's result. The allowable load repetition is found from the stress ratios. The actual load repetition is found by multiplying the load repetition factor by the expected number of departures.

The pavement could sustain infinite load repetition if the stress ratio is less than 0.51. The percentage fatigue which is found by dividing the actual by allowable load repetition should be less than 1. The structural capacity in each iteration of trial thickness is found until it is less than 1. As a general rule, the slab's longer length should not be more than twenty-four times the slab thickness, according to the PCA.

4.1.3. Evaluation of load stress - modified Westergaard's method

Westergaard's approach for determining maximum stresses in concrete pavement is based on thin-plate theory, with a single slab supported on a Winkler foundation and the load model considered to be an equivalent single-wheel load (ESWL). Based on thin plate theory, Westergaard's formulas for calculating the maximum bending tensile stress in a single-concrete slab owing to a single-wheel load with a circular or semi-circular contact area are provided for three loading conditions: slab-interior, edge, and corner. The necessary permissible bending tensile stress at the key slab loading places is determined by including the landing gear load in these formulae. Westergaard's formula for maximum bending stress in slab interior is given by

$$\sigma_i = \left(\frac{3(1+m)P}{2\pi h^2} \right) \left[In \frac{l}{b} + 0.6159 \right] \tag{2}$$

Where, P= ESWL;

p=contact pressure;

Where the relative stiffness radius '*l*' is provided by,

$$l = \left[\frac{Eh^3}{12k\left(1-m^2\right)} \right]^{0.25} \tag{3}$$

Where, the radius of tyre contact area, $a = \sqrt{\frac{P}{p\pi}}$ (4)

$b = a$ **when a** $\geq$ **1.724h** (5)

$b = \sqrt{1.6a^2 + h^2 - 0675h}$ **when, a<1.724h** (6)

Ioannides et al (1985) modified the equations given by Westergaard for edge stress as shown in Eq (7).

For a circular load region, the maximum edge bending tensile stress 'c' at the slab top at the angle bisector at a certain distance is given by,

$$\sigma_{e^c} = \left(\frac{3\left(1+m\right)P}{\pi\left(3+m\right)h^2} \right) \left\{ In\left[\frac{12\left(1-m^2\right)l^4}{100a^4} \right] + 1.84 - \frac{4m}{3} + \frac{1-m}{2} + \frac{1.18\left(1+2m\right)a}{2l} \right\} \tag{7}$$

Where, the radius of tyre contact area, $a = \sqrt{\frac{2P}{p\pi}}$ (8)

4.1.4. Evaluation of temperature stress - Eisenmann's method

When limited by the slab's self-weight, temperature difference induces curling and warping, resulting in thermal stress production. This is because the slab is unable to maintain a complete connection with the substructure. Thermal stress models for the given research region take into account linear temperature gradients. Eisenmann also suggested stress models owing to the temperature gradient in a slab with limited dimensions, which are based on the idea of critical slab length (lcrit). It is more appropriate than Bradbury's thermal stress solution since it considers both the partial contact of the slab with the supporting soil and the foundation stiffness. It is assumed that the temperature stress at the slab edge is 85% of the temperature stress at the slab centre in the same direction.

Three cases are observed based on the relationship between slab length 'L' and critical contact length 'l_{crit}',

L<l - Due to warping, the slab only contacts the subgrade in four corners.

L=l - At the four corners and the slab centre, the slab comes into contact with the

subgrade.

$L>l$ - The subgrade is in interface with the longer central part of the slab.

The generalized Eisenmann's temperature at the slab interior is given by,

$$\sigma_{\Delta t}^{i}=\left[\frac{L'}{0.9l_{crit}}\right]^{2}\frac{E\alpha\Delta t}{2(1-\mu)}\ \textbf{for}\ \left(L'<0.9l_{crit}\right) \tag{9}$$

Where,

h = thickness of the slab,

Δt =T/h=temperature difference

k = Winkler's reaction modulus;

μ = Poisson's ratio of concrete

The slab spanning 'L" is always smaller than the slab length L and is specified as such.

by, $L'=L-\left(\frac{2C}{3}\right)$ (10)

The support length 'C' is given b

$$C=4.5\sqrt{\frac{h}{k\Delta t}} \tag{11}$$

The critical length valid for $L=L_{crit}$ *or* $\mathbf{L>1.1}L_{crit}$ is given by,

$$l_{crit}=22.8h\sqrt{E\alpha\Delta t}\ \textbf{for square slab} \tag{12}$$

$$l_{crit}=20\sqrt{E\alpha\Delta t}\ \textbf{for rectangular slab} \tag{13}$$

The temperature gradient corresponding to the study area is applied in Eisenmann's Eq(10) to find the warping stresses for the edge and interior. IRC: 58-2002 Specifications for rigid pavement design for highways may be used to calculate the temperature gradient. The edge stress is taken to be 85 % of interior temperature stress. The mathematical addition of Westergaard's load and Eisenmann's temperature stress yields the total stress.

4.1.5. Method of finite element static analysis

As a basis, an elastic half-space was assumed, and the impact of fluctuations in Young's modulus was investigated in comparison to Winkler's reaction modulus. Temperature variations and different gear positions of A-310 and A-380 aircraft were investigated. The simulation model is

made up of 3D homogeneous, isotropic rectangular-shaped slabs of concrete sitting evenly on the sub-base and foundation layer. The stresses caused by the A-380's TRDT landing gear design are evaluated. It is comparable to the TADT landing gear layout of the A-310. The temperature difference (linear) readings were entered into the ANSYS model at the slab's top and bottom surfaces. For greater precision, the meshing is done in three levels. To determine the most detrimental bending tensile stress values, the landing gear-loading location on the concrete slab is taken into account. Simulations are run at several loading positions, such as D1-slab centre, D2-tangential to the length of the slab, D3-slab corner, and D4-tangential to the contraction-expansion joint. The weight of the aeroplane is transferred to the concrete slab as equally distributed loads in a quasi-elliptical surface. It takes more time to calculate, thus an equivalent rectangular loading area with a tyre impression of length Le is used. Fig. A2 depicts the flowchart (APPENDIX-B).

4.1.5.1. Locations of slab loading

To determine the most detrimental bending tensile stress values, the landing gear-loading location on the concrete slab must be examined. Numerous simulations were conducted at multiple load positions, such as D1-slab centre, D2-tangential to slab length, D3-slab corner, and D4-tangential to the contraction-expansion joint. The D2 loading position produces the greatest bending tensile stress values, it is found (Figs. 2-4).

4.1.5.2. Tyre impression loading area

The appropriate rectangular tyre impression area =0.5227 Le^2;

Rectangle area length =0.8172(Le);

Rectangle width area = 0.6 L.

4.1.6. Comparative analysis

Comparative analysis may be done between the stress resultants obtained from Finite Element Modelling using ANSYS and those of Modified Westergaard’s method. The percentage variation in stresses between the two methods is found, based on which the structural parameters such as slab thickness and concrete properties having less anomaly are chosen.

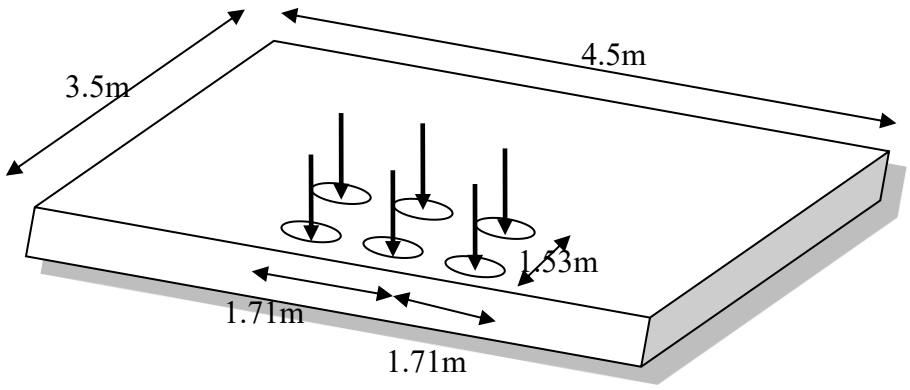

Fig. 2. Airbus 310 - Loading land Gear in D2 Location.

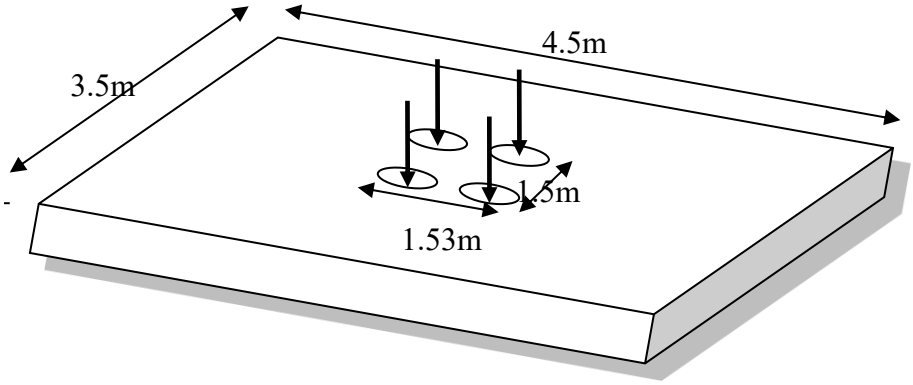

Fig. 3. Airbus 310 - Loading land Gear in D3 Location.

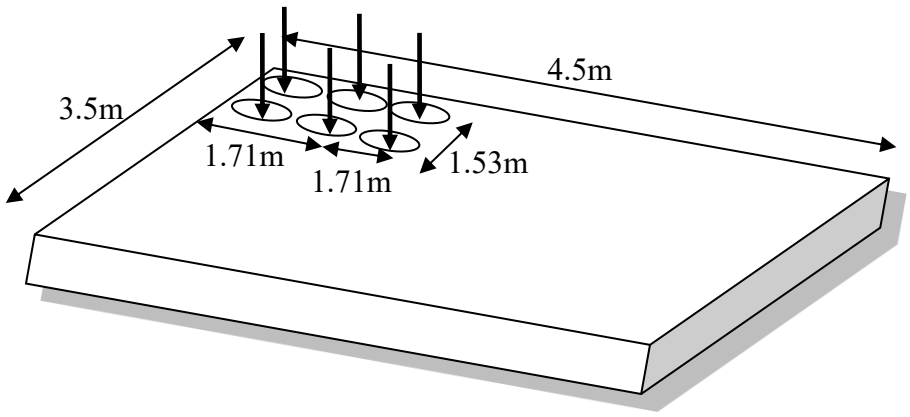

Fig. 4. Airbus 310 - Loading land Gear at D4 Location.

5. Results and discussion

5.1. Problem statement

The Mangalore International Airport located in Karnataka state is having an existing concrete runway pavement of length 2450 m, making it difficult for wide-body aircraft such as B-777 and A-380 to avail of their services. Hence a proposal for new cement concrete pavement for which the structural aspects such as thickness and material properties are to be modelled and analysed. The total number of Annual Aircraft Movements is around 10759 flights/year. The following design parameters are considered:

Modulus of subgrade reaction for the supporting soil	=	8 kg/cm^3
Flexural strength of the concrete slab	=	40 kg/cm^2
Average day and night temperature at peak summer	=	45˚C and 22˚ C.
Concrete's thermal expansion coefficient	=	10X10^{-6}/˚C
Existing pavement length and width	=	2450 m, 200 m.
Soil type	=	Red laterite, clayey soil
Design aircrafts considered	=	A-310 , A-380
Tyre pressure of the Design aircraft-310	=	1.2MPa
Tyre pressure of the Design aircraft-380	=	1.5MPa
The design life of pavement structure	=	20 years

The sampling value for the static analysis of the proposed runway is chosen as follows: The strength properties of parametric concrete are selected from conventional strength concrete (M25, M30), high strength concrete (M60), and very high strength concrete (M100). The present heavy-weight aircraft which is availing its service from Mangalore is A-310, having tandem dual wheel landing gear configuration chosen as the critical aircraft. The comparison study is effected by considering A-380 as the future wide-body aircraft (critical aircraft) to avail of its service. It has a tridem dual wheel landing gear configuration.

5.2. Flight data analysis and thickness determination using FAA method

Here the determination of equivalent annual departure of critical aircrafts A-310 and A-380 using FAA-specified landing gear conversion factors as specified in Table 1 and Eq(1) is done, thereby converting all other departing aircraft in terms of the design aircraft's landing gear configuration. The initial reference trial thickness for the proposed portion of the runway is obtained using FAA's design chart. This is illustrated in Table 3 and Table 4 for critical aircraft of A-310 (present) and A-380 (future).

5.2.1. Calculation of initial reference design thickness using FAA design chart

Annual Equivalent Departure by Critical Aircraft A-310	=	5531
Flexural Strength of Concrete, M	=	40kg/cm²
A factor of Safety, fos	=	1.75
Design Modulus of Rupture, (M/fos)	=	40/1.75 = 22.86kg/cm²

Cement Treated Base Course Thickness = 150 mm
Based On the FAA Design Chart Thickness h = 31.75 cm
In non-critical areas (0.9h) = 28.575 cm

Using the flight departure statistics obtained from AAI's annual report, the equivalent annual departure in terms of design aircraft A-310 and A-380 by the FAA method is predicted. After applying FAA's suitable conversion factors, the landing gear configurations of different aircraft are represented in terms of standard A-310 and A-380 configurations. The equivalent annual departure is found to be 5531 and 3507 for A-310 and A-380 as discussed in Table 3 and Table 4 respectively. Using this design critical departure and further static and dynamic analysis could be affected. Further, the initial trial design thickness was found to be around 31.75 cm, based on which the positive and negative thickness parametric iterations such as 20cm, 25cm, 30cm, 35cm, and 40 cm are made. These iterations are made to find the most structurally capable slab thickness for a given aircraft loading, which will be discussed in further study.

Design aircraft = Airbus-310
Landing gear configuration of critical aircraft = dual tandem

Load/Wheel (kg) of critical aircraft, w1=16970 kg

Table 3
Mangalore Airport-Departing Air-traffic data and Calculation of Equivalent Annual Departure in terms of Design Aircraft A-310.

Aircraft Types	Departure (20yrs.)	Gear Type	R (to Dual Tandem)	Load/Wheel (kg)	(w2/w1)^0.5	Log(R2)	Log(R1)	R1
Airbus 321	6719	dual	0.6	21233	1.12	3.61	4.03	4032
ATR 72-300	9599	dual	0.6	5147	0.55	3.76	2.07	5759
Airbus 310	19200	dual tandem	1	16970	1.00	4.28	4.28	19200
Airbus 319	8644	dual	0.6	15295	0.95	3.71	3.53	5186
Boeing 737-800	12483	dual	0.6	18820	1.05	3.87	4.08	7490
Airbus 330-200	32646	dual tandem	1	27420	1.27	4.51	5.74	32646
Boeing 737-700	40320	dual	0.6	16698	0.99	4.38	4.35	24192
Boeing 737-900R	13467	dual	0.6	20275	1.09	3.91	4.27	8080
Bombardier Dash 8	6724	dual	0.6	34258	1.42	3.61	5.12	4034
							Total	110619

Source: Mangalore airport flight departure statistics-Equivalent annual dept. in terms of Design Aircraft = 110619/20 = 5531 Flights per year

Design aircraft = Airbus-380

Landing gear configuration of critical aircraft = dual tridem

Load/Wheel (kg) of critical aircraft, w1=67880 kg

Table 4
Mangalore Airport-Departing Air-traffic data and Calculation of Equivalent Annual Departure in terms of Design Aircraft A-380.

Aircraft Types	Departure (20 yrs.)	Gear Type	R (to Dual Tridem)	Load/Wheel (kg)	(w2/w1)^0.5	log(R2)	log(R1)	R1
Airbus 321	6719	dual	0.33	21233	0.67	3.35	2.25	2217
ATR 72-300	9599	dual	0.33	5147	0.33	3.50	1.16	3168
Airbus 380	19200	dual tridem	1	46867	1.00	4.28	4.28	19200
Airbus 319	8644	dual	0.33	15295	0.57	3.46	1.97	2852
Boeing 737-800	12483	dual	0.33	18820	0.63	3.61	2.29	4119
Airbus 330-200	32646	dual tandem	0.57	27420	0.76	4.27	3.27	18608
Boeing 737-700	40320	dual	0.33	16698	0.60	4.12	2.46	13306
Boeing 737-900R	13467	dual	0.33	20275	0.66	3.65	2.40	4444
Bombardier Dash 8	6724	dual	0.33	34258	0.85	3.35	2.86	2219
							Total	70133

Source: Mangalore airport flight departure statistics-AAI

Equivalent annual dept. in terms of Design Aircraft = 70133/20

=3507Flights per

5.3. Check for structural capacity of the runway– PCA method

Assume the initial trial thickness of the slab, h = 30 cm.

Table 5
Determination of Structural Capacity of Slab Thickness by PCA method.

Aircraft Types (1)	Stress lbs./in² (2)	Stress Ratio (3)	Expected no. of Departure (4)	Load Repetition Factor (5)	Fatigue Repetition (6)	Allowable no. of Repetition (7)	Structural Capacity % (8)
Airbus 321	28	0.7	6719	0.28	1881.38	2000	0.94
ATR 72-300	15	0.375	9599	0.05	479.94	0	infinity
Airbus 310	19	0.475	19200	0.33	6335.87	0	infinity
Airbus 319	22	0.55	8644	0.33	2852.44	130000	0.02
Boeing 737-800	30.2	0.755	12483	0.13	1622.83	490	3.31
Airbus 330-200	33	0.825	32646	0.33	10773.07	360	29.93
Boeing 737-700	27.8	0.695	40320	0.13	5241.60	2500	2.10
Boeing 737-900R	31.7	0.7925	13467	0.13	1750.72	160	10.94
Bombardier Dash 8	26.72	0.668	6724	0.25	1680.99	6000	0.28
						Total	47.52

Design thickness of pavement satisfying check for structural capacity, h= 30 cm=11.81 inches.

Table 5 gives the flexural stress values found from corresponding PCA design charts, based on which the allowable load repetition in column-7 of Table 5 is found. The actual load repetition in column-6 of Table 5 is found by multiplying the load repetition factor by the expected number of departures. The percentage fatigue in column-8 is found by dividing the actual by allowable load repetition, the total summation of which is found to be 47.52 % which is less than 100 %(fatigue criteria given by PCA). Further for this structurally capable pavement, the initial trial thickness is found to be around 30cm, which is in close correlation with FAA's design thickness.

5.4. Determination of maximum allowable stresses by modified Westergaard's method

5.4.1. Calculation of equivalent single wheel load using load calculation number method

1. For A-310:

Undercarriage load of the A-310	=	67 tonnes
Equivalent Single Wheel Load (ESWL)	=	$\frac{\text{The total load on one undercarriage}}{\text{reduction factor}}$
Axle to Axle distance for dual tridem arrangement	=	1.53 m
The total contact area of wheels under one undercarriage or landing gear	=	8100 cm²
The total load on one undercarriage	=	67000 kg
Reduction factor(LCN graph)	=	3.2
ESWL	=	20312.5 kg

2. For A-380:

Undercarriage load of A-380	=	165 tonnes
Equivalent Single Wheel Load	=	$\frac{\text{The total load on one undercarriage}}{\text{reduction factor}}$
Axle to Axle distance for dual tridem arrangement	=	1.7 m
The total contact area of wheels under one undercarriage	=	10998 cm²
The total load on one undercarriage	=	165000 kg
Reduction factor	=	3.3
ESWL	=	50000kg

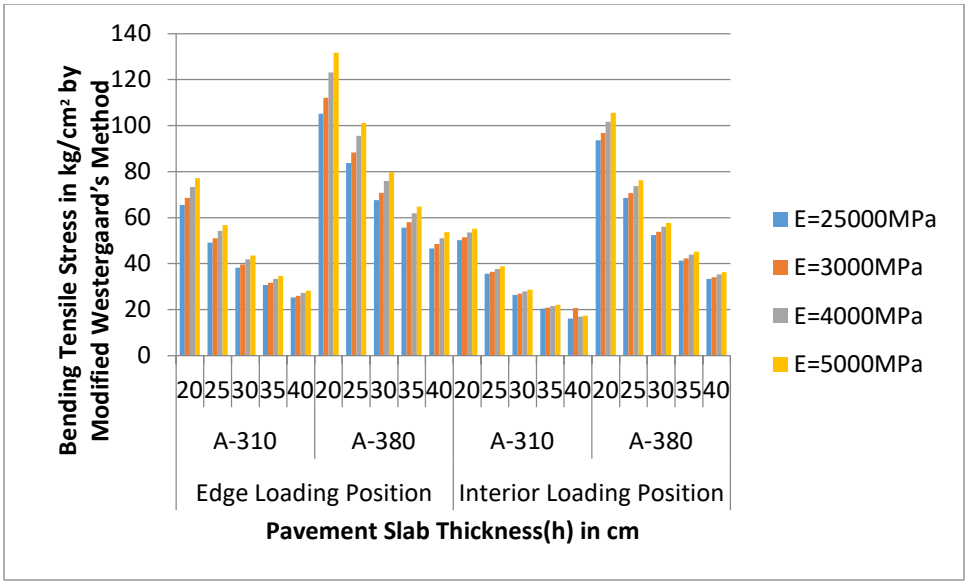

Fig. 5. Bending Tensile Stress values for A-310 and A-380 at Edge and Interior Region by Modified Westergaard's Method

The ESWL for A-310 and A-380 is calculated as specified in the LCN method, based on which it is found to be 20312.5 kg and 50000kg. Fig. 5 presents the variation in edge and interior stress values for the thickness and elastic modulus parameters for the two design aircraft considered. There is a prominent increase in stress values with the decrease of slab thickness and increase of elastic modulus values and this increment is widely visible from A-310 to A-380's load which explains its correlation with Hooke's law. As far as the comparison is concerned with the edge and interior stress values, edge stresses stand greater in magnitude accounting for the edge boundary condition, as specified by the FAA method.

5.5. Calculation of limiting allowable warping stress by Eisenmann's method

Based on Mangalore city's day and night temperature variation at peak summer the average night and day temperatures were taken to be 22˚C and 45˚ C. The slab temperature differential values were taken based on Table 6.

Table 6
Slab Temperature Differential Values for Mangalore.

Slab thickness, h (cm)	Temperature differential (/˚C)
20	19
25	20.3
30	21
35	22
40	23.5

Source: IRC 58-2011 Design Specifications for Plain Jointed Cement Concrete Pavements

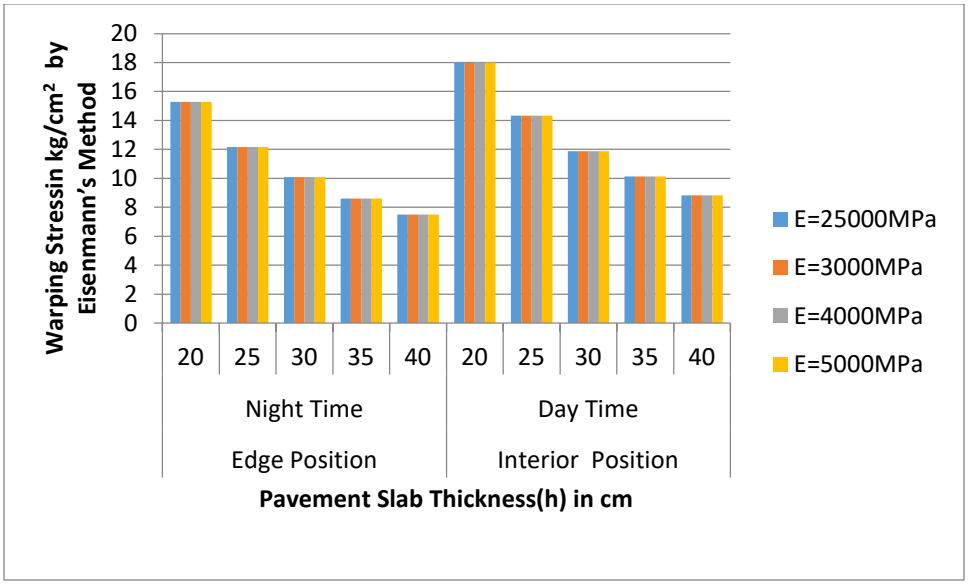

Fig. 6. Edge and Interior Region Warping Stress by Eisenmann's Method.

Eisenmann's method is compared to conventional Bradbury's method for temperature stress calculation, as it makes use of critical slab length which it makes on warping and curling as the temperature differential within the slab thickness varies. Fig. 6. shows that the warping stress values are found to decrease with a thickness which better explains Bradbury's law. This explains the fact that with increasing slab thickness there is a suitable decrement in the warping stress values.

A C-program for finding the maximum warping stress of the extended pavement is written based on the boundary condition (refer to APPENDIX A, APPENDIX B)

5.6. Determination of static load bending tensile stress using FEM (ANSYS)

Finite element meshing is performed on all three levels of every concrete slab model. The element type chosen is 8 node-solid 185. The distance between the transverse and longitudinal joints of a single slab-Jointed plain concrete pavement (slab width and length) is considered to be 3.5m and 4.5m respectively as per Table 2. The coefficient of thermal expansion of the concrete is taken to be 1x 10^{-5} mm/mm/˚C.

Table 7
Input Parameters Considered in the Finite Element Modelling of Slab.

Layer	Elastic modulus, E (MPa)	Poisson's ratio(μ)	Layer Density(γ)
concrete slab	25000 , 30000, 40000 , 50000	0.15	2.40E-03
sub base	144.158	0.3	6.00E-04
subgrade	17.1616	0.4	3.00E-04

The slab thickness is taken to be 25cm, 30cm, 35cm, and 40cm considering iterations of 5 cm. Four concrete kinds with moduli of elasticity of 25000MPa, 30000MPa, 40000MPa, and 50000MPa as specified in Table 7 are chosen, and a Poisson's ratio of 0.15 is used. The Airbus A-380 has the heaviest take-off weight and the most complicated landing gear. Because of the greater distance between the landing gears, the effect of each landing gear is considered independently. The gross take-off weights of the A-310 and A-380, which are transmitted through TADT and TRDT landing gears, are P = 67500kg and P = 165000kg, respectively. The comparable rectangular area of wheel loading is calculated for matching tyre pressures of A-310 and A-380 based on the tyre imprint loading as specified in the calculation below. These wheel loads are given to the nodal points while taking axle spacing and wheel spacing into account.5.5.1 Determination of tyre contact area for a given landing gear configuration.

Table 8
Tyre contact area for a given landing gear configuration.

	for Airbus–310	for Airbus–380
Tyre pressure in kg/cm^2	12	[15]
Load on one landing gear in tone	67.88	165
Load on 1 tyre in kg	16970	41250
Tyre imprint area in cm²	1414.167	3437.5
$0.5227L^2$	1414.167	3437.5
L^2	2705.503	6576.43
L in cm	52.01445	81.09
$0.6L$ in cm	31	49
$0.8712L$ in cm	45	71

Thus, tyre impression areas of 31 cm x 45 cm and 49 cm x 71 cm are achieved for the A-310 and A-380 landing gear configurations, respectively.

The static analysis of the proposed pavement is done for edge and interior landing gear locations and the results as shown in Fig. 15. The warping stress due to temperature is found by suitably referring to the temperature differential between the top and bottom of the pavement surface for the Mangalore area given as per IRC’s codal provision and shown in Fig. 16.

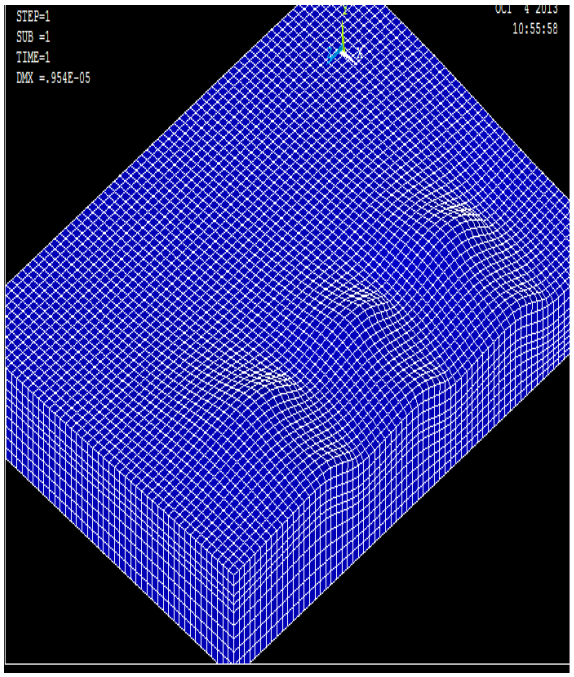

Fig. 7. Pavement model showing Displacement for Airbus 380 - Landing Gear in D2 Loading Position.

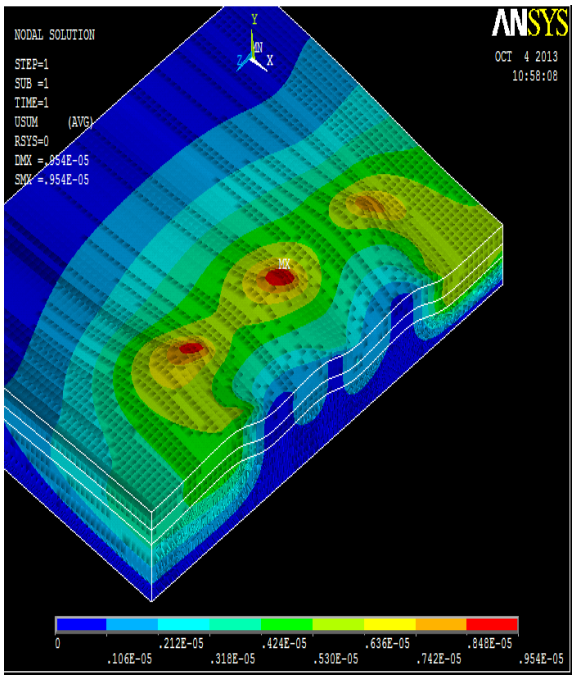

Fig. 8. Pavement model showing Stress variation forAirbus380-Landing Gearin D2 Loading Position.

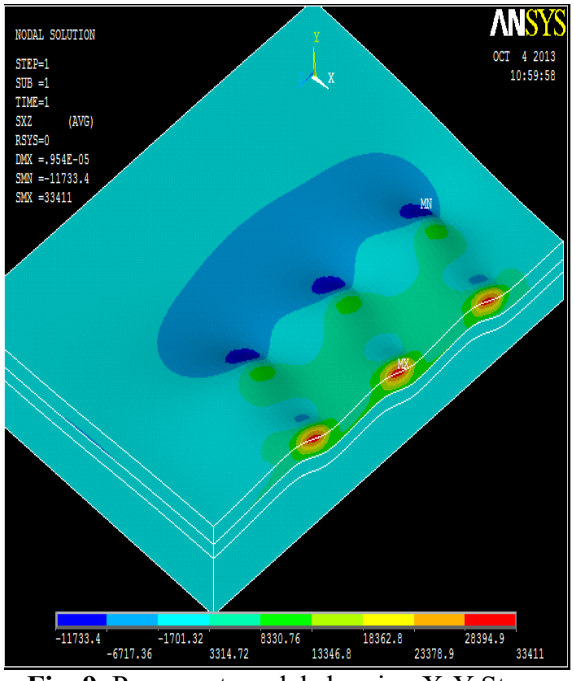

Fig. 9. Pavement model showing X-Y Stress variation for Airbus 380 - Landing Gear in D2 Loading Position.

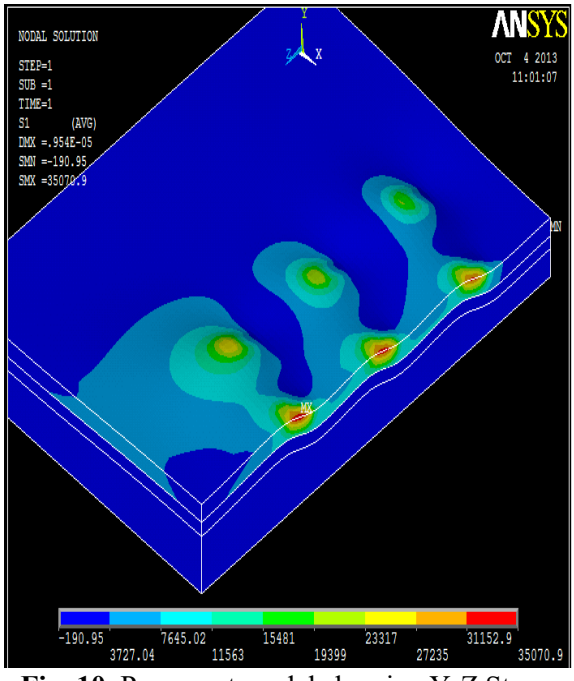

Fig. 10. Pavement model showing Y-Z Stress variation for Airbus 380 - Landing Gear in D2 Loading Position

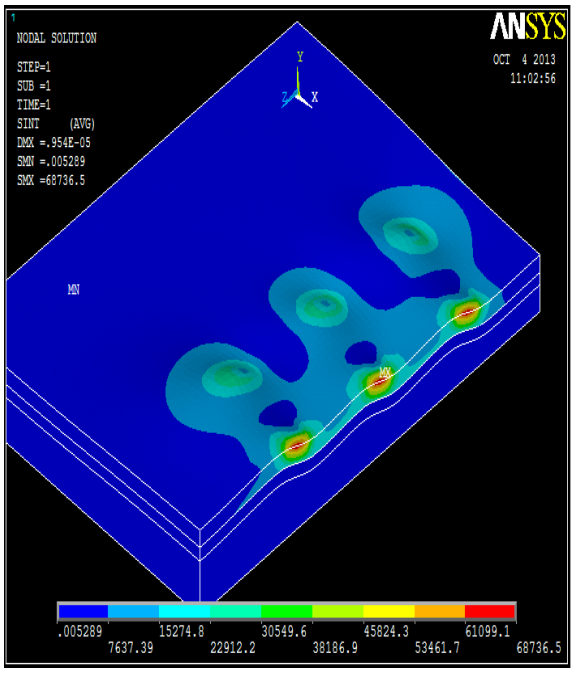

Fig. 11. Pavement model showing X-Z Stress variation for Airbus 380 - Landing Gear in D2 Loading Position.

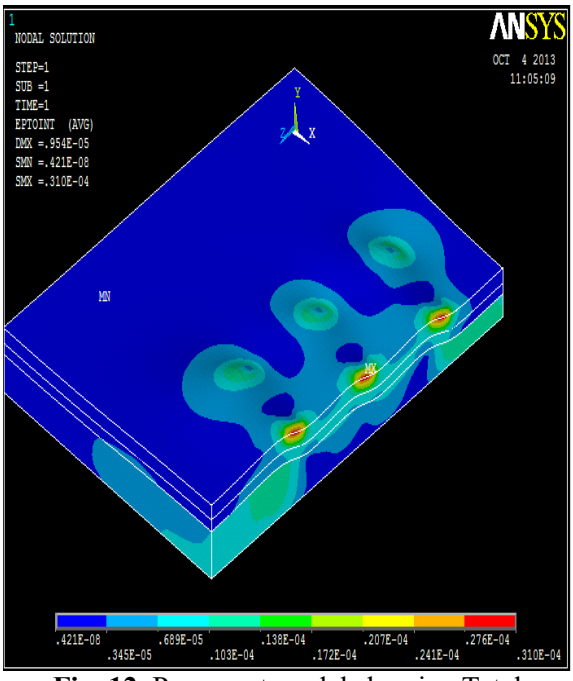

Fig. 12. Pavement model showing Total Mechanical Strain Intensity variation for Airbus 380 - Landing Gear in D2 Loading Position.

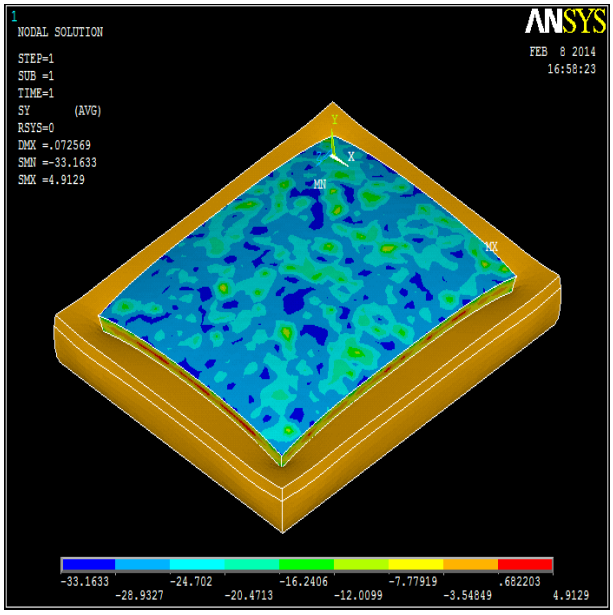

Fig. 13. Pavement model showing Warping of the slab due to Temperature variation (Day time).

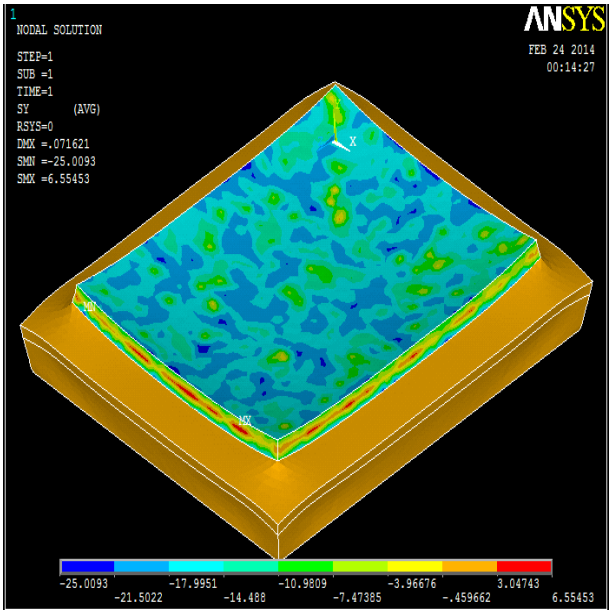

Fig. 14. Pavement model showing Warping of the slab due to Temperature variation (Night time).

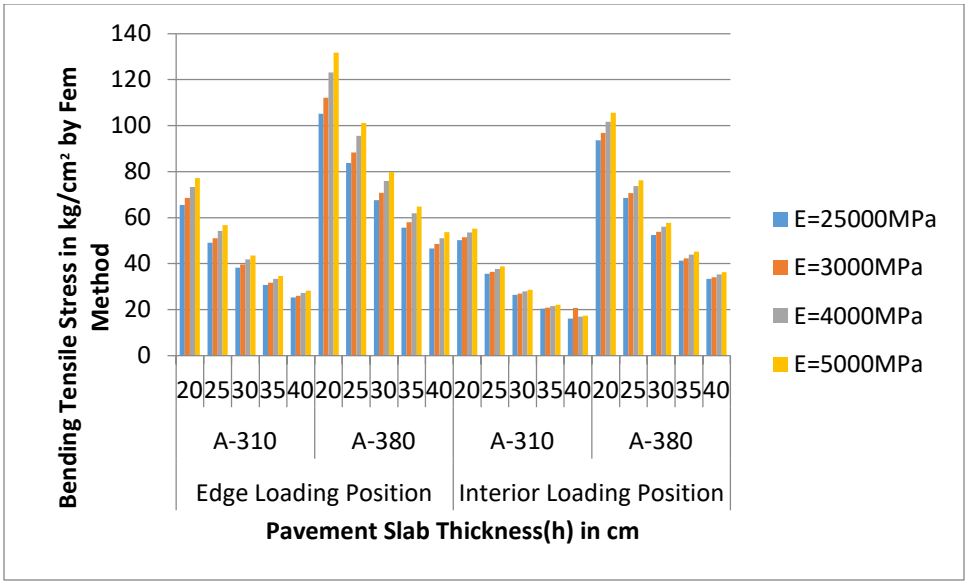

Fig. 15. Edge and Interior Region Load Stresses by FEM.

Fig. 7 depicts the finite element meshing of the airfield pavement resting on a 150 mm thick sub-base over a homogeneous subgrade. Fig. 8 to Fig. 12 present the variation of stress resultants namely, shear stress with stress components in all directions. From Fig. 15 it is found that using ANSYS for finite element modelling of rigid airfield pavement for D2 and D3 loading position of tandem and tridem-dual tyre configuration of landing gears i.e., of A-310 and A-380, the stress values were found to vary with increasing thickness and with concrete' property i.e., the elastic modulus of concrete. For the D2-edge loading condition for aircraft A-310, the bending tensile stress values were found to vary from 20.34 to 83.50 kg/cm^2. For the same condition, the stress values inculcated by A-380 aircraft range from 28.58 to 124.3kg/cm^2. The least values were for those conventional or standard strength concrete having an Elastic modulus of 25000 MPa and the highest values were found to belong to high strength concrete having an Elastic modulus of 50000 MPa. For the D3-interior loading condition for aircraft A-310, the bending tensile stress values were found to vary from 19.46 to 70.12kg/cm^2. For the same condition, the stress values inculcated by A-380 aircraft range from 29.56 to 105.4 kg/cm^2. The least values were for those conventional or standard strength concrete having an Elastic modulus of 25000 MPa and the highest values were found to belong to high strength concrete having an Elastic modulus of 50000 MPa. The limiting maximum values of bending tensile stress found from both edge and interior landing gear loading positions were found to increase significantly with rises in elastic modulus and compressive strength values of concrete and to reduce concurrently with increases in pavement slab thickness.

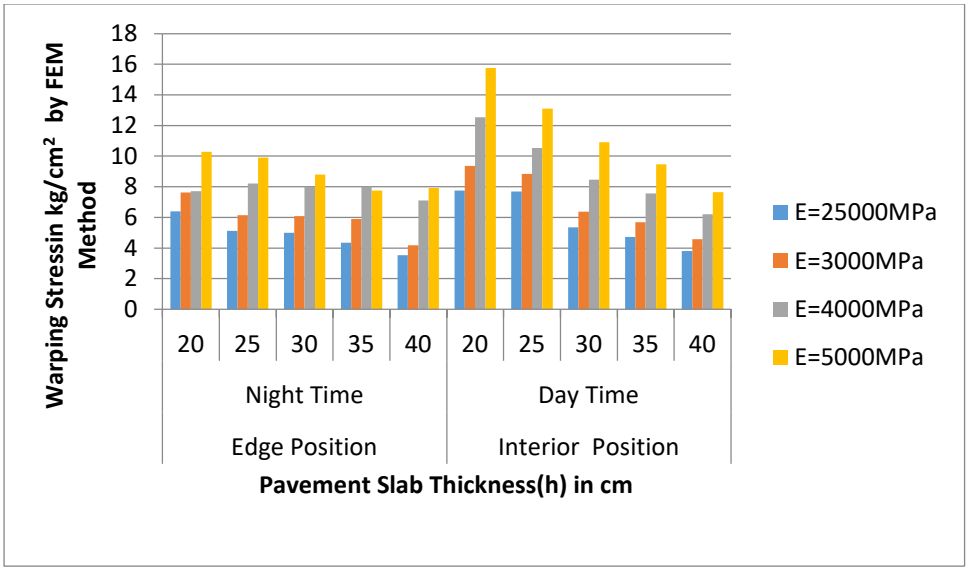

Fig. 16. Edge and Interior Region Warping Stress values by FEM.

The slab is examined for both + temperature gradients (temperatures at the top of the slab are greater than those at the bottom) and -temperature gradients (the temperature at the bottom of the slab is higher than that at the top). The temperature is expected to vary linearly over the depth of the slab. The slab deflects more near the corner than within. Figs 17 and 18 demonstrate the deflected form for this situation of + temperature gradient temperature. In terms of slab length and thickness, a + curling temperature gradient produces higher stress than a - curling temperature gradient. As can be seen in Fig. 16, as the temperature gradient increases, so does the stress. For a slab thickness of 20 cm, the maximum negative curling stress is 10.293 kg/cm^2. Fig. 17 illustrate the deflected form for - and + temperature gradient.

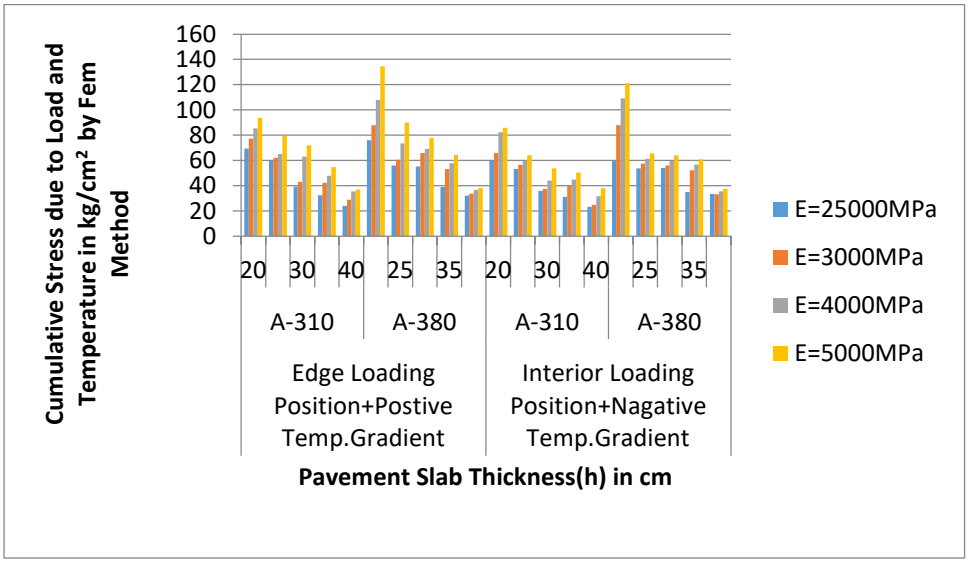

Fig. 17. Cumulative Stress values due to Load and Temperature (FEM).

From Fig. 15 it was found that using ANSYS for finite element modelling of rigid concrete pavement for D2 and D3 loading position of tandem and tridem-dual tyre configuration of landing gears i.e., of A-310 and A-380, the total stress values were found to vary with increasing thickness and with varying concrete' property i.e., the elastic modulus of concrete. The restrictive highest values of bending tensile stress found from both edge and interior landing gear loading locations were discovered to significantly rise with rises in elastic modulus and compressive strength values of concrete and to reduce concurrently with rises in pavement slab thickness.

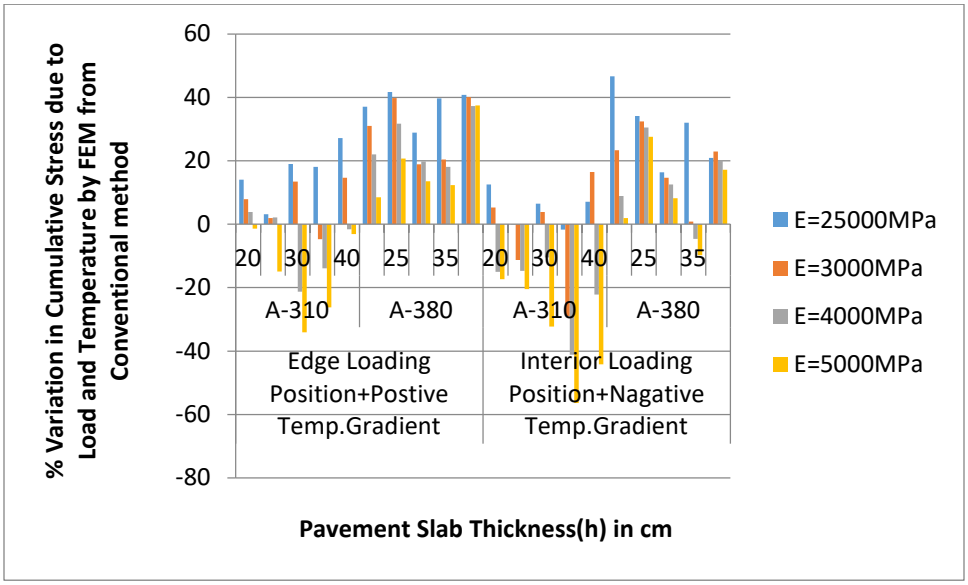

Fig. 18. % Variation in Stress Values by FEM from the Conventional method.

The results of ANSYS and Theoretical Westergaard's method are compared in Fig. 18. It shows the variation of additive values of stress for edge load is found to be around 1.01% to 37.10 %. The variation of additive values of interior load stresses with positive stress gradients is found to be around 7.345% to 26.18%. The variation of additive values of edge load with negative temperature gradient is found to vary from 12.37%-41.71 %.

For interior load stresses with a positive temperature gradient, it is found to be around 1.92% to 46.63%. Based on these results, the anomaly in stress variation between the conventional method and FE model using ANSYS was found to be much reduced in concrete type having modulus of elasticity value E = 30000 MPa i.e. M40 and slab thickness lying between 30 cm and 35 cm. This inference is justified by its proximity in relevance with design thickness as obtained by the FAA method initially.

6. Conclusions

A good runway should fulfil the structural requirements in addition to the geometry of the runway design. In this approach, it is important to pay greater attention to pavement slab analysis and design. Using the Finite Element Method vs. Closed-Form Solution, this study established the structural static response features, such as the thickness and the concrete characteristics, for

the newly proposed rigid airport runway pavement. The numerous research findings are covered as follows.

- Using finite element modelling of rigid airfield pavement for D2 and D3 loading of A-310 and A-380, the stress values are found to increase with the thickness and elastic modulus of the concrete.
- From both the outside and inside landing gear loading positions, the maximum values of bending tensile stress were found to go up a lot as the concrete's elastic modulus and compressive strength went up, but they went down at the same time as the thickness of the pavement slab went up.
- For the D2-edge loading condition of the aircraft A-310, the bending tensile stress is determined to be lowest for conventional-strength concrete with an elastic modulus of 25000 MPa, and greatest for high-strength concrete with an elastic modulus of 50000 MPa. An identical trend was seen in the A-310 and A-380 D3-interior loading circumstances.
- When tested for both positive and negative temperature differences, the slab deflected greater at the corner than in the interior. A positive curling temperature difference causes greater stress than a negative curling temperature difference. It was determined that when the temperature difference grows, so does the stress.

Funding

This research received no external funding.

Conflicts of interest

The authors declare no conflict of interest.

References

[1] Taheri MR, Zaman MM. Effects of a moving aircraft and temperature differential on response of rigid pavements. Comput Struct 1995;57:503–11. https://doi.org/10.1016/0045-7949(94)00625-D.

[2] Report F. FAA Finite Element Design Procedure for Rigid Pavements. Security 2007.

[3] Patil VA, Sawant VA, Deb K. Use of finite and infinite elements in static analysis of pavement. Interact Multiscale Mech 2010;3:95–110. https://doi.org/10.12989/imm.2010.3.1.095.

[4] Wadkar A, Mehta Y, Cleary D, Zapata A, Musumeci L, Kettleson W. Effect of Aircraft Gear Positions and Gear Configurations on Load Transfer Efficiency of Airfield Rigid Pavement Joints. Road Pavement Mater. Charact. Model. Maint., Reston, VA: American Society of Civil Engineers; 2011, p. 40–8. https://doi.org/10.1061/47624(403)6.

[5] Cai J, Wong LNY, Yan HW. Dynamic Response of Airport Concrete Pavement to Impact Loading. Adv Mater Res 2012;594–597:1395–401. https://doi.org/10.4028/www.scientific.net/AMR.594-597.1395.

[6] Yadav DK, Nikraz H. TECHNICAL EVALUATION OF A RUNWAY USING THE DEFLECTION METHOD. Aviation 2013;17:150–60. https://doi.org/10.3846/16487788.2013.861647.

[7] Shafabakhsh G, Kashi E, Tahani M. Analysis of runway pavement response under aircraft moving load by FEM. J Eng Des Technol 2018;16:233–43. https://doi.org/10.1108/JEDT-09-2017-0093.

[8] Rezaei-Tarahomi A, Kaya O, Ceylan H, Kim S, Gopalakrishnan K, Brill DR. Development of rapid three-dimensional finite-element based rigid airfield pavement foundation response and moduli prediction models. Transp Geotech 2017;13:81–91. https://doi.org/10.1016/j.trgeo.2017.08.011.

[9] Yi-Qiu T, Yong-Kang F, Yun-Liang L, Chi Z. Responses of snow-melting airfield rigid pavement under aircraft loads and temperature loads and their coupling effects. Transp Geotech 2018;14:107–16. https://doi.org/10.1016/j.trgeo.2017.11.006.

[10] Xu B, Zhang W, Mei J, Yue G, Yang L. Optimization of Structure Parameters of Airfield Jointed Concrete Pavements under Temperature Gradient and Aircraft Loads. Adv Mater Sci Eng 2019;2019:1–11. https://doi.org/10.1155/2019/3251590.

[11] Liu P, Wang C, Lu W, Moharekpour M, Oeser M, Wang D. Development of an FEM-DEM Model to Investigate Preliminary Compaction of Asphalt Pavements. Buildings 2022;12:932. https://doi.org/10.3390/buildings12070932.

[12] Rezazadeh Eidgahee D, Jahangir H, Solatifar N, Fakharian P, Rezaeemanesh M. Data-driven estimation models of asphalt mixtures dynamic modulus using ANN, GP and combinatorial GMDH approaches. Neural Comput Appl 2022;34:17289–314. https://doi.org/10.1007/s00521-022-07382-3.

[13] Zhao Y, Jiang J, Zhou L, Ni F. Improving the calculation accuracy of FEM for asphalt mixtures in simulation of SCB test considering the mesostructure characteristics. Int J Pavement Eng 2022;23:80–94. https://doi.org/10.1080/10298436.2020.1733566.

[14] Ge H, Quezada JC, Houerou V Le, Chazallon C. Multiscale analysis of tire and asphalt pavement interaction via coupling FEM–DEM simulation. Eng Struct 2022;256:113925. https://doi.org/10.1016/j.engstruct.2022.113925.

Appendix A.

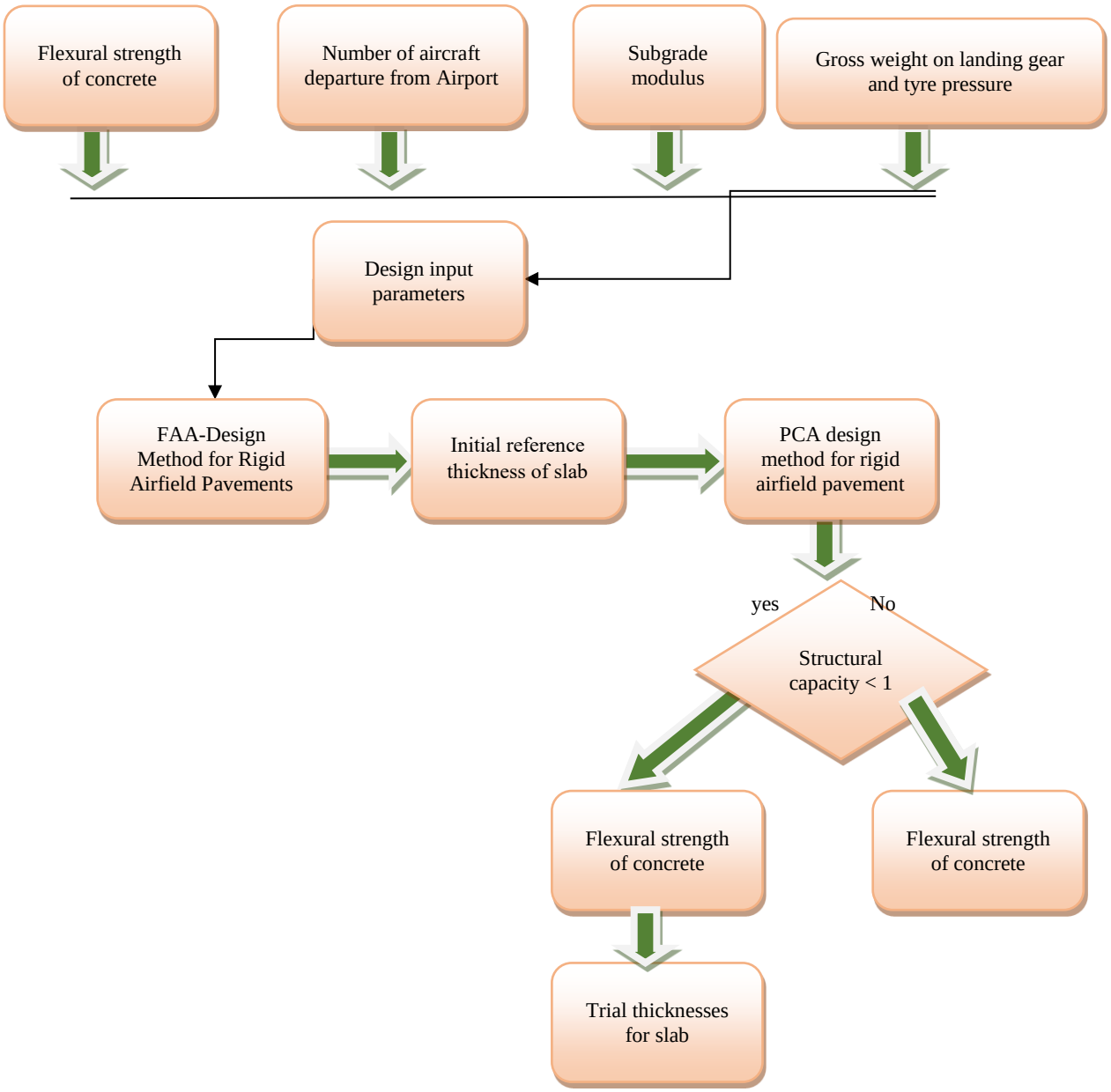

Fig. A1. Evaluation of reference thickness for the proposed pavement.

Appendix B.

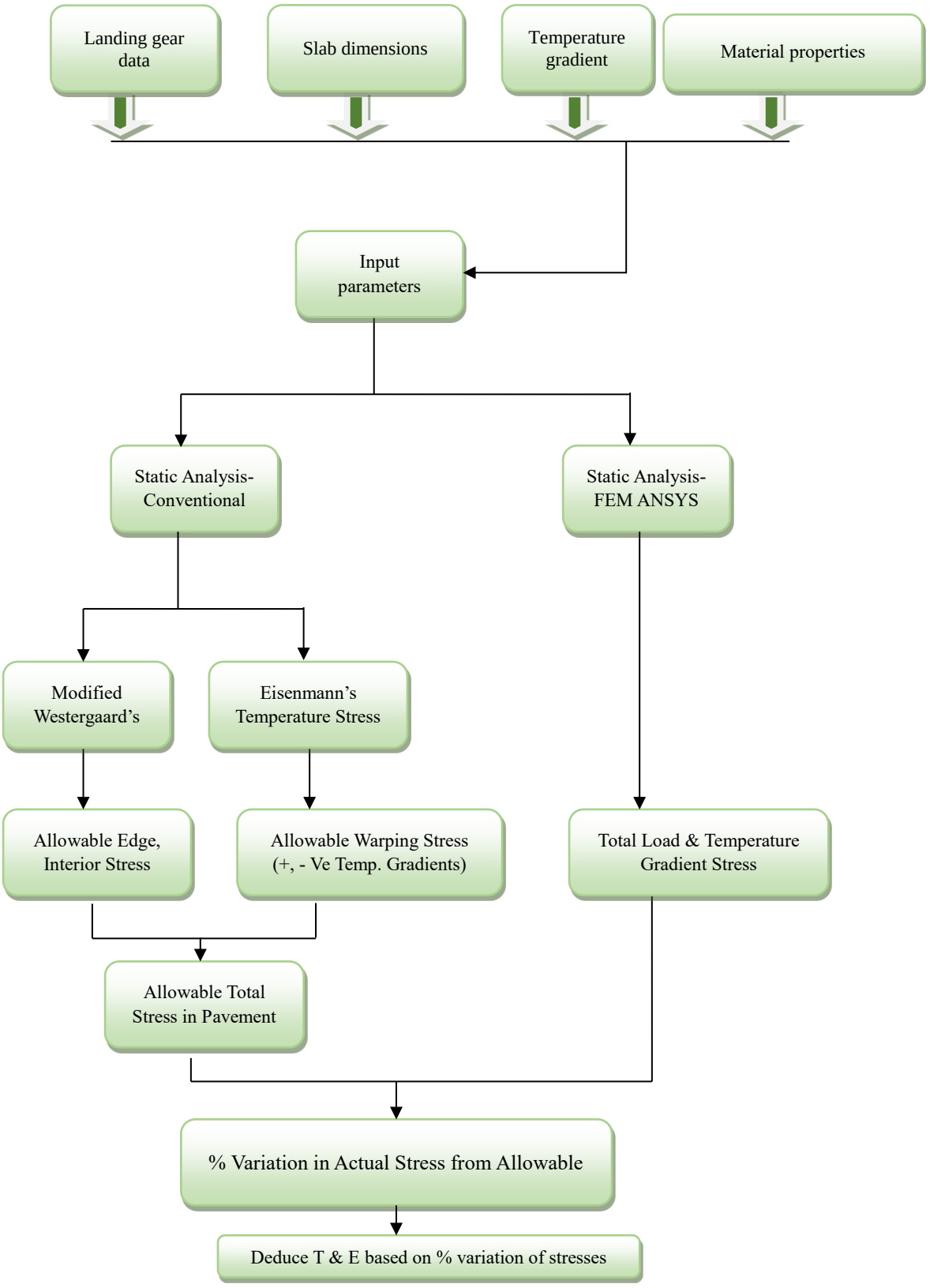

Fig. A2. Calculation of thickness and modulus of elasticity for static stresses using traditional and FEM.